J. Embryol. exp. Morph. **89**, 159–173 (1985)
Printed in Great Britain © *The Company of Biologists Limited 1985*

Cell distributions in the retinal ganglion cell layer of adult Leptodactylid frogs after premetamorphic eye rotation

S. A. DUNLOP AND L. D. BEAZLEY

Neurobiology Laboratory, Department of Psychology and Neuromuscular Research Institute, Queen Elizabeth II Medical Centre, University of Western Australia, Nedlands, Australia 6009

SUMMARY

In adult *Limnodynastes dorsalis* and *Heleioporus eyrei* regions of high cell density in the retinal ganglion cell layer are normally found along the nasotemporal axis and become apparent only after metamorphosis (Dunlop & Beazley, 1981; Coleman, Dunlop & Beazley, 1984). Eye rotations were performed from embryonic to mid-larval life and cell topography mapped after metamorphosis using cresyl violet-stained wholemounts. Mature cell distributions indicated that from stages equivalent to 30/31 in *Xenopus* (Nieuwkoop & Faber, 1956) alignment of high cell density regions had already been determined and developed to reflect the degree of eye rotation. We conclude that cell topography in the adult ganglion cell layer is determined from the time at which invagination of the eye cup nears completion. Furthermore, the correspondence in adults between alignment of high cell density regions and the orientation of the visuotectal projection suggests that these features could not be dissociated by manipulation of the developing eye.

INTRODUCTION

In many adult vertebrates, cells in the retinal ganglion cell layer are arranged in specialized patterns (reviewed Stone, 1981). The adult frog *Limnodynastes dorsalis* possesses a nasotemporally aligned visual streak within which lies a temporally situated area centralis of highest cell density. Also, in adults of a closely related species *Heleioporus eyrei*, there are high density regions in nasal and temporal retina within a distinct visual streak. These patterns contrast with *Xenopus laevis* in which density gradients across the mature retina are shallow. In all these species adult cell distributions first become apparent in juveniles, the topography before metamorphosis being essentially radial with low central densities (Dunlop & Beazley, 1981, 1984; Coleman *et al.* 1984).

In this study we have analysed mature cell distributions in the ganglion cell layer of *Limnodynastes* and *Heleioporus* after premetamorphic eye rotations. Thus we have tested whether adult cell topography is determined from stages of development before such specializations are apparent. Furthermore, we assessed

Key words: eye rotation, development, visual streak, frog, area centralis.

visuotectal projections electrophysiologically in *Limnodynastes*, anticipating them to be rotated, since the developing eye anlage already contains information in terms of future central connections (Gaze, Feldman, Cooke & Chung, 1979; Sharma & Hollyfield, 1980; Humphrey, Dunlop & Beazley, 1980). Therefore, to investigate whether cell density gradients in the ganglion cell layer arise independently of factors which determine central projections, we have compared alignment of the area centralis and visual streak with that of the visuotectal projection. Some of this data has been published in abstract form (Dunlop, Humphrey, Coleman & Beazley, 1983).

METHODS

Animals and surgery

Limnodynastes egg masses were collected from King's Park and Lake Gwellup, Perth in June–August. Staging was by equivalence to eye development in *Xenopus laevis* (Nieuwkoop & Faber, 1956; Grant, Rubin & Cima, 1980) as assessed from 1 μm Epon/Araldite toluidine blue-stained sections of whole embryos fixed in 0·067 M-phosphate-buffered 2·5 % glutaraldehyde. Osmication, dehydration and embedding procedures have been described elsewhere (Beazley & Dunlop, 1983). Transverse sections are shown at the level of the optic stalk and/or optic nerve (Fig. 1). *Heleioporus* larvae were collected from Kardinya, Perth in August and staged by equivalence to limb development in *Xenopus* (Nieuwkoop & Faber, 1956). Earlier stages of *Heleioporus* proved difficult to rear under laboratory conditions.

Surgery was performed at stages equivalent to NF 28/29–40 for *Limnodynastes* (n = 24) and NF 53/54 for *Heleioporus* (n = 8) (Nieuwkoop & Faber, 1956). Embryos, removed from their jelly coats, and larvae were washed several times in 50 % Holtfreter's solution before being transferred to dishes with plasticene supports and containing 100 % Holtfreter's solution with 0·15 % MS222. Using standard techniques (Gaze *et al.* 1979; Munro & Beazley, 1982) unilateral eye rotations of 45°, 90° or 180° were performed for left eyes in *Limnodynastes*, and of 45° or 90° for right eyes in *Heleioporus*. Only at earliest stages was it necessary to sever the optic stalk. At later stages care was taken to leave the optic stalk/nerve intact. Such a procedure was followed since optic nerve section in late larval amphibia (Beazley, 1981) and in adults (Beazley, Darby & Perry, 1985; Humphrey & Beazley, 1985) has been shown to lead to death of some retinal ganglion cells. Three hours after surgery animals were transferred to 50 % Holtfreter's solution for several days before being placed in spring water.

Operated animals, along with unoperated controls, were maintained as described previously (Coleman *et al.* 1984). *Limnodynastes* were raised for 8–10 months after metamorphosis to allow development of an area centralis (Beazley & Dunlop, unpublished observations). However,

Fig. 1A–E. Lateral view of normal *Limnodynastes* embryos representing stages at which unilateral eye rotations were performed. For each stage the corresponding degree of eye development is shown in coronal section with the diencephalon to the left; dorsal is up. (A) NF stage 28/29. Invagination has progressed to the equator and the lens placode (*lp*) has thickened; *os* indicates the optic stalk. (B) NF stage 30/31. Invagination is almost complete in ventral retina and the pigment epithelium (*pe*) is in full contact dorsally. The retina is concave and the lens rudiment (*l*) is not fully detached from the overlying ectoderm. Arrows indicate optic axons leaving the eye ventrally. (C) NF stage 32/33. A lens cavity has appeared and the lens is now detached. Fascicles of axons (arrows) are well developed in the optic stalk (*os*). (D) NF stage 37. The lens cavity is a thin slit and embraces the inner wall of the lens. A diffuse inner plexiform layer (*ipl*) and clear optic nerve (arrow) are seen. (E) NF stage 40. The retinal layers are distinguishable, the lens cavity has disappeared and mesenchyme (*m*) is continuous as the inner cornea. Arrow indicates the optic nerve approaching the chiasm. Toluidine blue, 1 μm sections. Scale bars: animals – 1 mm; all sections 50 μm.


1A

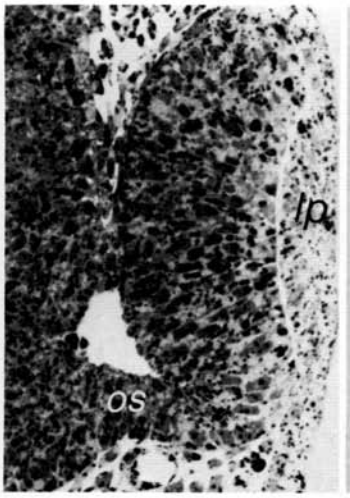
os


C

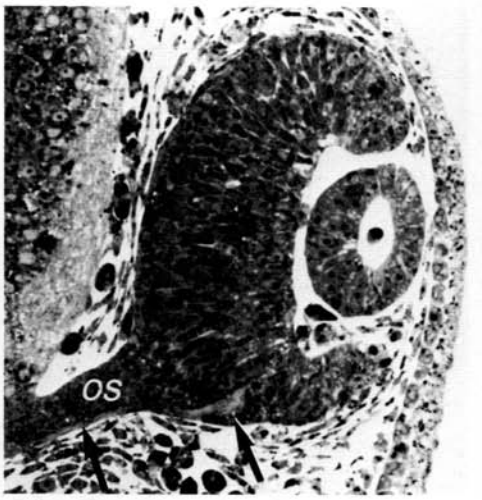
os


B


os


D

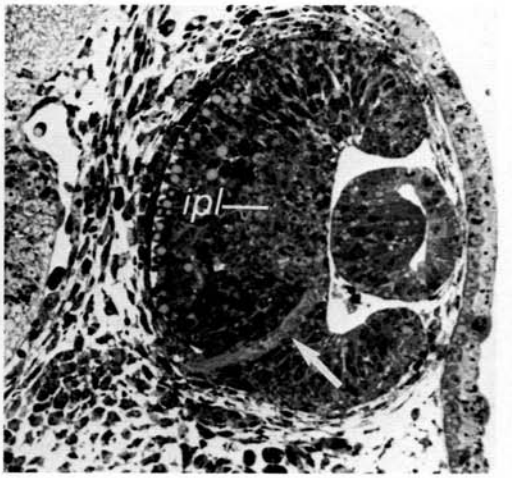
ipl


E

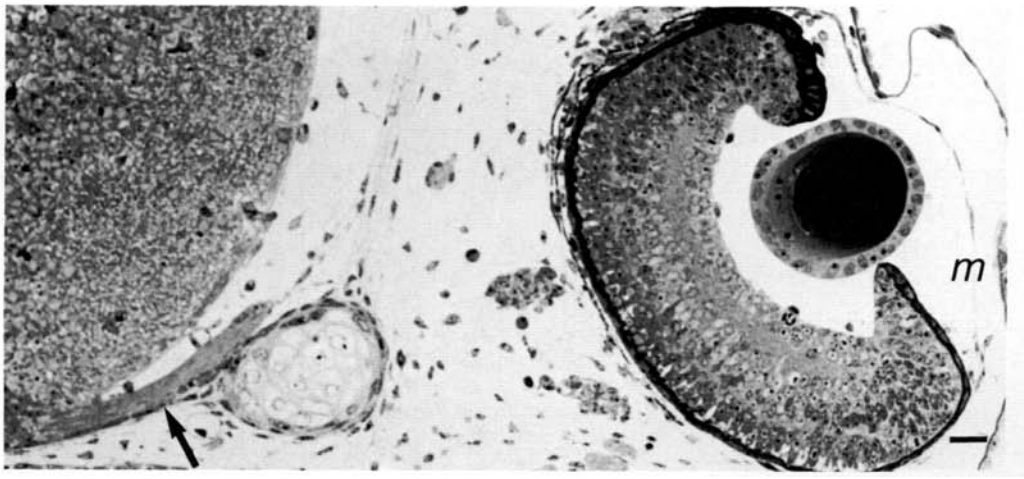
m

Heleioporus was maintained after metamorphosis for only 2–3 months since by this time an essentially adult-like pattern with high cell density regions nasally and temporally would normally have developed (Dunlop & Beazley, 1981). Animals were checked at weekly intervals and discarded if the operated eye had derotated, as assessed by comparison with the unoperated eye in which the choroid fissure with associated hyaloid artery was ventral. Derotation of the operated eye occurred in four *Limnodynastes* and three *Heleioporus*.

Previous studies of eye development have suggested that extensive cell death may result from surgical procedures at early stages, with subsequent growth of a new and therefore necessarily unrotated eye (Jacobson, 1978; Gaze *et al.* 1979; reviewed Beazley, 1984). We checked that similar confounding factors had not taken place in our experiments by fixing *Limnodynastes* embryos at 3 h (n = 3), 3 d (n = 3) and 21 d (n = 3) after 180° eye rotation and examining tissue as toluidine blue-stained semithin sections.

Visuotectal mapping

Limnodynastes were anaesthetized by immersion in a 0·1 % solution of MS222. Prior to mapping, the region between the back of the eye and optic chiasm was observed through a slit in the skin of the roof of the mouth. Animals in which an optic nerve from the operated eye could not be seen were not mapped (n = 11, representing animals operated at all stages). For those animals with a clear optic nerve, visuotectal projections were recorded from the operated eye to the contralateral tectum using standard electrophysiological techniques (Munro & Beazley, 1982). We do not report electrophysiological data for *Heleioporus* in which anaesthesia diminished or abolished responses.

Histology

After electrophysiological mapping in *Limnodynastes*, but before recovery from anaesthesia, the optic nerve on the experimental side was sectioned between the eye and optic foramen and a saturated solution of horseradish peroxidase (HRP, Sigma, type VI) applied. Twenty four hours later, under terminal anaesthesia with Nembutal (0·5 ml gm^{-1} body weight), eyes were removed for wholemounting and brains for HRP processing. Eyes were oriented with a dorsal cut, removed and fixed for at least one week in 10 % buffered formalin (pH 7·4). Retinal wholemounts, ganglion cell layer uppermost, were prepared and stained with cresyl violet (Dunlop & Beazley, 1981, 1984; Coleman *et al.* 1984). Shrinkage, determined from pre- and poststaining retinal areas, did not exceed 11 %. Whole brains, with their meninges removed, were processed fresh in 0·08 % diaminobenzidine and 0·1 % hydrogen peroxide. Tissue was fixed in 10 % buffered formalin and optic pathways examined as whole brain preparations. In *Heleioporus*, retinal wholemounts were prepared as for *Limnodynastes*.

Analysis of wholemounts

As with our previous studies (Dunlop & Beazley, 1981, 1984; Coleman *et al.* 1984) we considered the total cell population of the ganglion cell layer since cell types were indistinguishable on morphological grounds in cresyl-stained wholemounts. Cell counts, excluding blood elements, were made per $(0{\cdot}1\,mm)^2$ sample area at ×1000 magnification.

We have previously reported and confirmed in this study that cells in the ganglion cell layer of normal adult *Limnodynastes* are arranged as a temporally situated area centralis of highest density within a visual streak of intermediate density extending into nasal retina. Densities were low ventrally and particularly dorsally (Coleman *et al.* 1984). In normal adult *Heleioporus* high density regions are found, as expected, both nasally and temporally (Dunlop & Beazley, 1981). Therefore, analysis of temporal, nasal, ventral and dorsal retina allowed alignment of high density regions to be determined in both species. In eyes with 90° or 180° rotation, their partner retinae and unoperated controls, up to eight sample areas were counted in these four key regions and mean values given (Tables 1 & 2). The exception was for eyes rotated by 45° in which alignment of high density regions was analysed by sampling temporoventral (TV), ventronasal (VN), nasodorsal (ND) and dorsotemporal (DT) regions. Nevertheless, in every case, the entire retina was surveyed to ensure that key areas reflected cell topography and that no regions with extremes of cell density were omitted by such sampling.

For retinae of both species, analysis of variance was used to test for significant differences in cell densities between regions. Since F proved to be significant ($P < 0{\cdot}01$) in every case, a planned orthogonal comparison was then used to test for significance between high and low density areas. In each case nasal & temporal regions were compared with dorsal & ventral. The exception was retinae rotated by 45° for which temporoventral & nasodorsal areas were compared with dorsotemporal & ventronasal. An additional comparison was made for *Limnodynastes* since highest cell densities are normally found in the temporally situated area centralis. Thus, temporal retina was compared with nasal in unrotated retinae and those rotated by 180°; in 90° rotated eyes a comparison of dorsal and ventral retina was made while values in temporoventral regions were compared with those in nasodorsal for eyes rotated by 45°.

Additional counts were made for two representative *Limnodynastes* retinae, a control and one in which the eye had been rotated by 180°. These wholemounts were systematically sampled at 5 % by area and isodensity contours drawn (Figs 3B, 4B).

Throughout, retinal locations are expressed in terms of the position of the eye within the head for both operated and unoperated retinae. Thus, after eye rotation, our convention reflects the eyes' eventual, rather than original, orientation.

RESULTS

Evaluation of embryonic surgery

In animals examined at 3 h, 3 and 21 days after eye rotation, operated eyes had not undergone degeneration. Indeed, as shown in Fig. 2A,B, embryonic surgery can result in a retina that by 3 days postoperatively had differentiated to a similar extent as the unoperated side. Therefore, we consider that in this study problems associated with complete degeneration of the eye anlage (Jacobson, 1978; Gaze *et al.* 1979; reviewed Beazley, 1984) were avoided. Furthermore, operated eyes showed signs of rotation. For example, 3 days after surgery the pattern of pigmentation in the pigment epithelium, although normally proceeding dorso-ventrally, progressed from the now ventrally placed pole of the eye; similarly, for operated retinae, the optic nerve exited dorsally with respect to the head rather than ventrally (Fig. 2A,B). Also, we noted that after metamorphosis in normal *Limnodynastes* and *Heleioporus* the circular pupil changed to a vertical slit and the initially black and gold iris developed predominantly black regions nasally and in particular temporally. Such features developed with an alignment which matched the degree to which the eye itself had been rotated (Fig. 2C).

Adult cell distributions and visuotectal projections

Cell densities for both retinae of three unoperated animals (two *Limnodynastes* and one *Heleioporus*) along with unoperated partner retinae of all nine experimental *Limnodynastes* and two of the three experimental *Heleioporus* were compared with results from rotated eyes. Furthermore, for each *Limnodynastes*, the visuotectal projection from the left eye to the right tectum was assessed.

(1) *Normal animals and unoperated eyes of experimental animals (Table 1)*

Cell morphology in the ganglion cell layer (Fig. 3A,B) was comparable to that previously reported (Dunlop & Beazley, 1981; Coleman *et al.* 1984). A minority of

cells had pale nuclei and clumped Nissl substance, thus fulfilling standard morphological criteria for identification as ganglion cells. By contrast, most cells were not recognizable as ganglion cells, being small with dark nuclei and sparse cytoplasm.

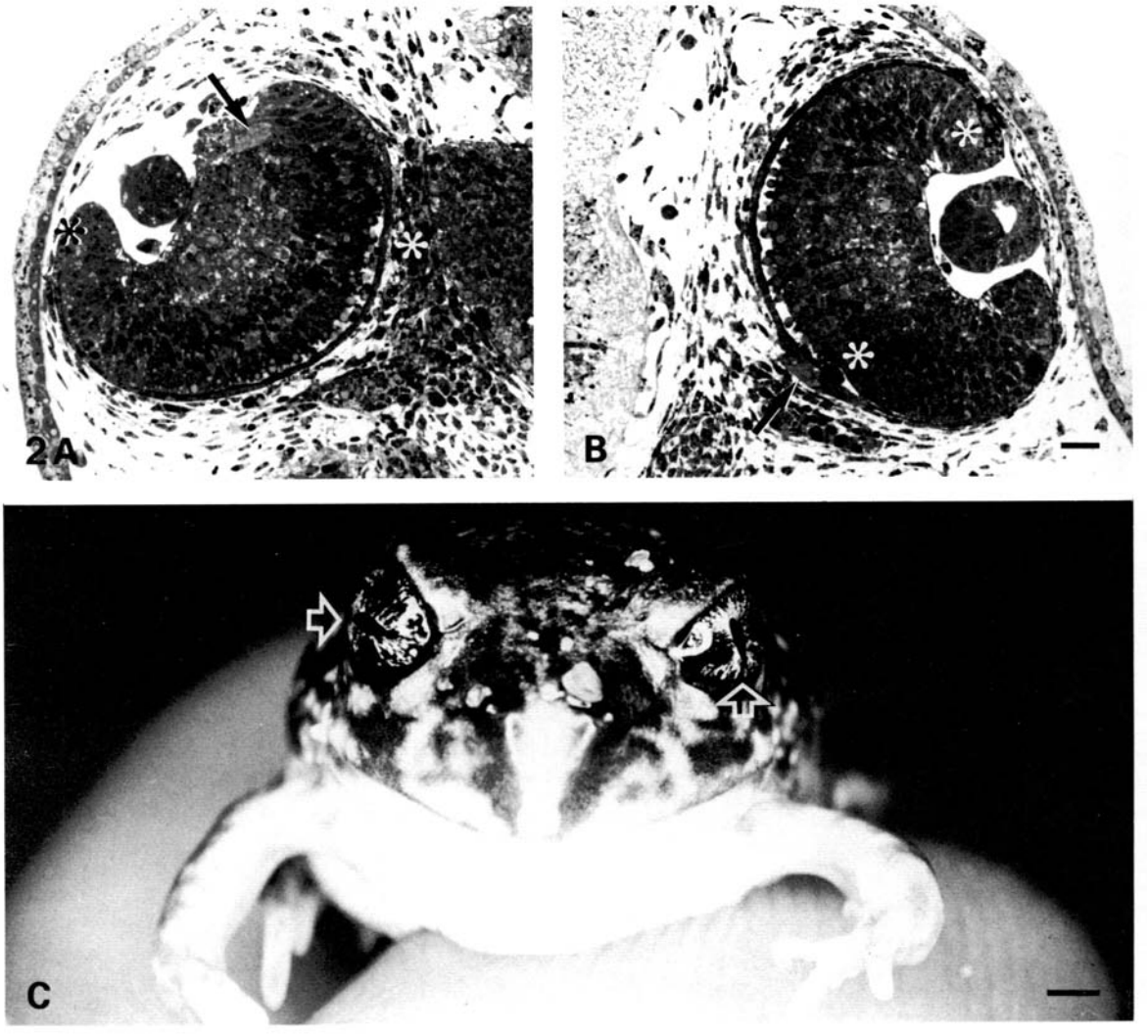

Fig. 2. (A,B) Micrographs of a coronal section of *Limnodynastes* eyes at NF stage 35; dorsal is up. The left eye (A) had been rotated by 180° 3 days previously, the right eye (B) is unoperated. Differentiation appears comparable and overlying ectoderm on the operated side has healed. The 180° rotation is evidenced by the dorsal as compared to normally ventral exit of the optic nerve (arrows) and by the position of pigmentation (between the asterisks): in the rotated eye pigment epithelium is seen ventrally whereas normally pigmentation is initiated in dorsal retina and proceeds towards the ventral pole. Toluidine blue, 1 μm sections. Scale bar: 50 μm. (C) Juvenile *Heleioporus* after rotation of its right eye by 90° clockwise at NF stage 53/54. The normally vertically oriented pupil (⌓) is horizontally aligned in the rotated eye (◊) and the black and gold iridial pigmentation is similarly rotated. Scale bar: 1 mm.

Table 1. *Summary of histological and electrophysiological data for normal* Limnodynastes *and* Heleioporus *for unoperated retinae of experimental animals*

Animal	T	D	N	V	p N&T v D&T	p N v T	Orientation of visuotectal projection
Normal animals							
LN1R	176	62	113	81	0·01	0·01	—
LN1L	190	72	122	86	0·01	0·01	normal
LN2R	173	58	112	80	0·01	0·01	—
LN2L	158	51	107	70	0·01	0·01	normal
HN1L	250	154	264	128	0·01	ns	—
HN1R	241	175	255	147	0·01	ns	—
Unoperated retinae of experimental animals							
LER1R	172	72	121	91	0·01	0·01	—
HER1L	222	147	196	136	0·01	ns	—
HER2L				retina not available			
LER8R	162	75	127	87	0·01	0·01	—
LER3R	176	69	133	90	0·01	0·01	—
LER6R	170	66	122	90	0·01	0·01	—
HER3L	181	97	192	91	0·01	ns	—
LER7R	174	59	112	76	0·01	0·01	—
LER9R	160	74	118	97	0·01	0·01	—
LER2R	172	87	133	107	0·01	0·01	—
LER4R	170	72	143	92	0·01	0·05	—
LER5R	119	58	85	76	0·01	0·01	—

Cell densities were sampled in temporal (T), dorsal (D), nasal (N) and ventral (V) regions described with respect to the head. Highest values (underlined) were seen in temporal retina of *Limnodynastes* and nasally and temporally in *Heleioporus*. L is left, R is right, p is the probability value of F for a planned orthogonal comparison. In cases marked —, visuotectal projections were not mapped; ns is not significant.

However, from our counts of axons in the optic nerve (Dunlop & Beazley, 1981; Coleman *et al.* 1984) we consider that a majority of cells in the ganglion cell layer of these species projected to the brain and therefore were ganglion cells.

For *Limnodynastes*, cell densities in temporal, nasal, ventral and dorsal retina ranged from 119–190, 85–143, 70–107 and 51–87 cells/$(0{\cdot}1\,\mathrm{mm})^2$ respectively. These values reflected the mature isodensity map which, as previously reported (Coleman *et al.* 1984) showed a temporally situated area centralis within a nasotemporally aligned visual streak (Fig. 3E). In *Heleioporus*, corresponding ranges were 181–250, 192–264, 91–147 and 97–175 cells/$(0{\cdot}1\,\mathrm{mm})^2$, compatible with the high density nasal and temporal regions previously described (Dunlop & Beazley, 1981). Variations in cell density between animals tended to reflect retinal area with lower values in larger retinae.

In both species cell densities in nasal and temporal regions were consistently significantly higher ($P < 0{\cdot}01$) than dorsally and ventrally. Also, in *Limnodynastes*, values in temporal retina were always significantly greater ($P < 0{\cdot}01$) than nasally.

Table 2. *Summary of histological and electrophysiological data for experimental animals*

Animal	°eye rotated	Stage operated	T	D	N	V	p N&T v D&V	p D v V	Orientation of visuotectal projection
LER1L	90°c	30/31	100	135	106	181	0·01	0·01	rotated 90°c
HER1R	90°c	53/54	133	205	180	238	0·01	ns	rotated 90°c
HER2R	90°c	53/54	106	178	125	199	0·01	ns	rotated 90°c
			TV	DT	ND	VN	TV&ND v DT&VN	TV v ND	
LER8L	45°c	29/30	104	55	108	65	0·01	ns	rotated 45°c
LER3L	45°c	32	176	63	125	88	0·01	0·01	rotated 45°c
LER6L	45°c	40	150	74	120	101	0·01	0·01	rotated 45°c
HER3R	45°c	53/54	114	209	124	222	0·01	ns	rotated 45°c
			T	D	N	V	N&T v D&V	N v T	
LER7L	180°	29/30	58	23	67	38	0·01	0·05	rotated 180°
LER9L	180°	30/31	36	22	38	21	0·01	ns	pattern 1
LER2L	180°	32	108	91	151	79	0·01	0·01	rotated 180°
LER4L	180°	37	78	48	168	24	0·01	0·01	rotated 180°
LER5L	180°	40	87	66	127	41	0·01	0·01	rotated 180°

In eyes rotated by 90° or 180°, temporal (T), dorsal (D), nasal (N) and ventral (V) retina was sampled. After 45° clockwise rotation, the regions analysed were temporoventral (TV), dorsotemporal (DT), nasodorsal (ND) and ventronasal (VN). Highest values, corresponding to the area centralis in *Limnodynastes* and the 2 high density regions in *Heleioporus*, are underlined. However, in LER8L and LER9L, 2 high values are underlined since although a weak visual streak appeared to have developed no clear area centralis had formed. After 90° clockwise, 45° clockwise or 180° rotations of the left eye in *Limnodynastes* the area centralis was found in ventral, temporoventral and nasal retina respectively. Following 90° clockwise or 45° clockwise rotations of the right eye in *Heleioporus* high density regions were found dorsally and ventrally or temporodorsally and nasoventrally respectively. Conventions are as in Table 1.

For normal *Limnodynastes* the primary projection to the dorsal part of the contralateral tectum was retinotopic and arose from superior field. Medial, lateral, rostral and caudal tectum respectively received input from superotemporal, inferonasal, superonasal and inferotemporal parts of this projection (Fig. 4A). HRP whole brain preparations showed optic axons to enter the brain at the chiasm, and terminate contralaterally in the tectum and basal optic nucleus as well as bilaterally in diencephalic visual centres, notably the corpus geniculatum thalamicum and neuropil of Bellonci.

(2) *Rotated eyes (Table 2)*

The morphology of cells in the ganglion cell layer of experimental retinae was essentially normal (Fig. 3C,D).

In seven experimental retinae cell densities were within (LER2L, LER3L, LER6L, HER2R and HER3R) or for one region slightly higher (LER1L and HER1R) than values in unoperated or normal eyes. In two further experimental

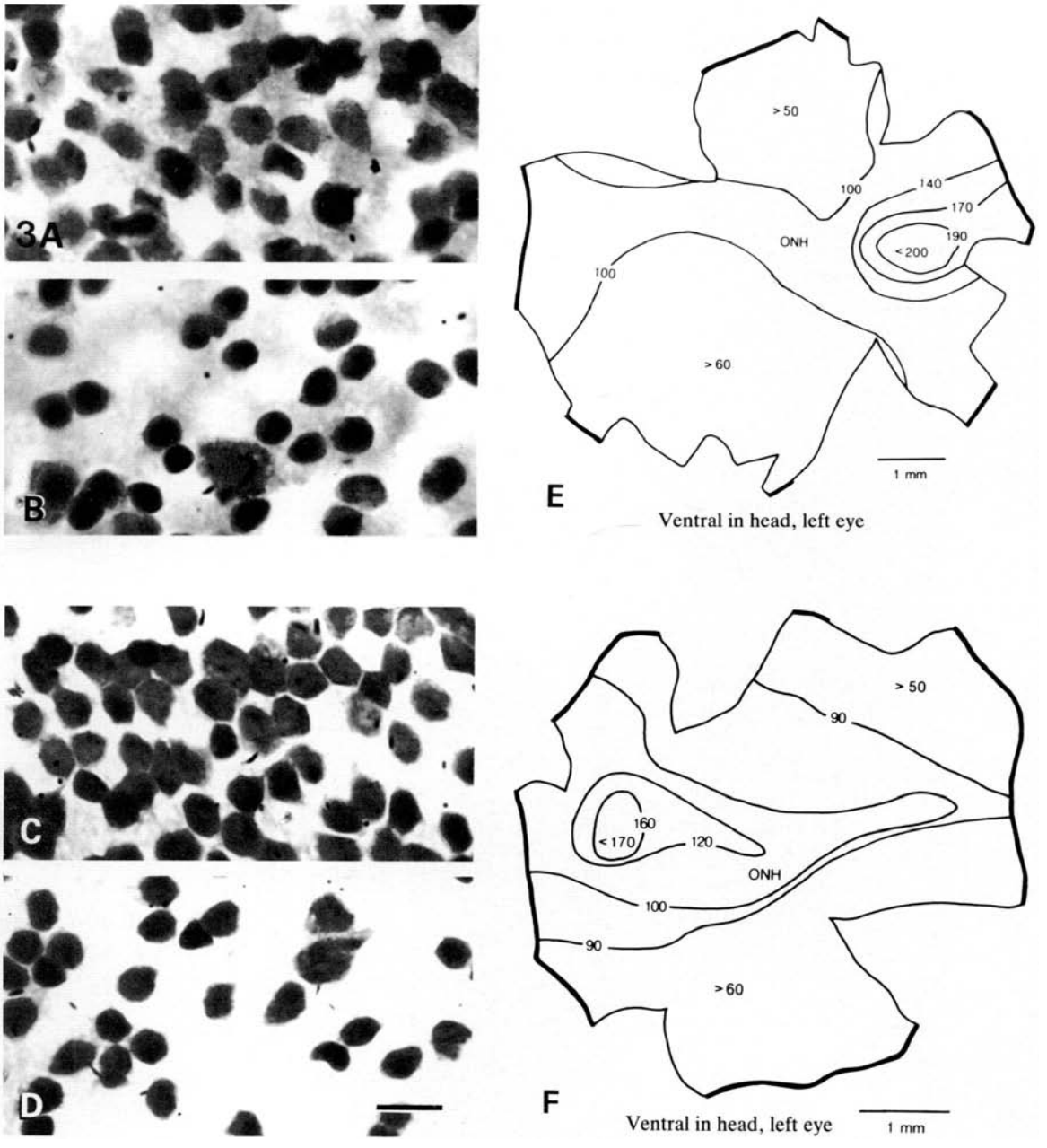

Fig. 3A–F. Retinal wholemounts for a normal *Limnodynastes* (A,B, & C) and after 180° eye rotation at NF stage 32 (C,D & F). (A–D) ganglion cell layer in high and low density regions. Cresyl violet. Scale bar: 10 μm. (E,F) isodensity maps of the total cell population in the ganglion cell layer of a normal *Limnodynastes* (E) and after 180° eye rotation (F). A region of highest cell density, the area centralis, is seen in temporal retina of the normal animal (E) but in nasal retina of the eye rotated by 180° (F). Numbers refer to cells per $(0{\cdot}1\,\text{mm})^2$ sample area. ONH is optic nerve head.

retinae (LER4L and LER5L) peak densities were comparable to unoperated or normal retinae although elsewhere values were somewhat lower. Three retinae (LER7L, LER8L and LER9L) had depleted cell densities.

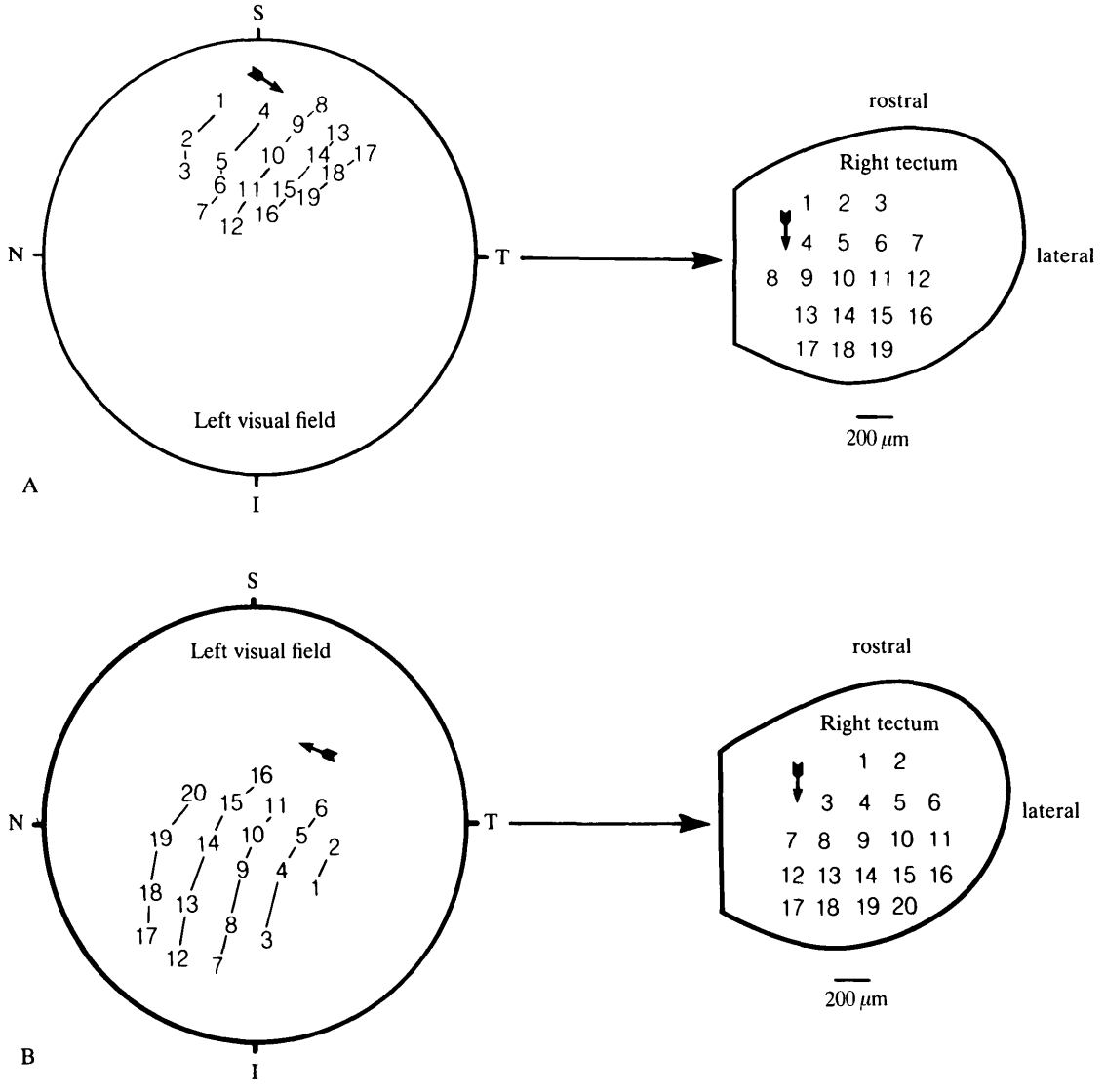

Fig. 4A,B. Electrophysiology. Visuotectal projection from the left eye (centred) to the dorsal part of the contralateral tectum in a normal *Limnodynastes* (A) and after 180° eye rotation (B). The visual field projections are as seen by an observer behind the perimeter arc and not as seen by the preparation. The boundary of each visual field extends 90° from the optic axis. Numbers indicate electrode placements on the tectum and their corresponding visual field positions which elicited maximal response. A rostrocaudal progression on the tectum results in a transition (small arrows) from superonasal towards inferotemporal visual field in the normal animal and from an inferotemporal to superonasal visual field after 180° eye rotation. S, I, T, and N are superior, inferior, temporal and nasal respectively. Scale bar: 200 μm.

In every case, cell densities indicated that specializations in the ganglion cell layer were rotated to the same extent as the eye itself. Thus, for example, after 90° clockwise rotations (LER1L, HER1R and HER2R) cell densities in dorsal and ventral retina were significantly higher ($P<0{\cdot}01$) than nasally and temporally. These results suggested that high density areas developed across the dorsoventral rather than the nasotemporal axis. Furthermore, for *Limnodynastes* LER1L, values ventrally were significantly higher ($P<0{\cdot}01$) than dorsally indicating that the area centralis had developed ventrally with respect to the head.

Rotations of 45° clockwise in *Limnodynastes* (LER8L, LER3L and LER6L) resulted in significantly higher ($P<0{\cdot}01$) densities temporoventrally & nasodorsally than dorsotemporally & ventronasally, indicative of high density regions across the temporoventral to nasodorsal axis. Additionally, two *Limnodynastes* with 45° clockwise rotations had significantly higher ($P<0{\cdot}01$) densities in temporoventral compared to nasodorsal retina, implying that the area centralis developed temporoventrally. For *Heleioporus* (HER3R) with a 45° clockwise rotation, the significantly higher ($P<0{\cdot}001$) values, dorsotemporally & ventronasally than elsewhere suggested the visual streak had developed across this axis.

The most prominent change after 180° rotation in *Limnodynastes* (LER2L, LER4L and LER5L) was seen in significantly higher ($P<0{\cdot}01$) cell densities in nasal rather than temporal retina. This data suggested that the area centralis developed in a nasal rather than the normal temporal location (Fig. 3F). As expected, cell densities in nasal and temporal retina were higher ($P<0{\cdot}01$) than dorsally and ventrally.

Rotated retinae of the three *Limnodynastes* which had developed abnormally low cell densities in the ganglion cell layer appeared nevertheless to have developed weak visual streaks. For two of these animals regional specializations appeared to be rotated. Thus, for LER8L, after a 45° clockwise rotation, significantly higher values ($P<0{\cdot}01$) were seen in temporoventral & nasodorsal retina compared to ventronasal & dorsotemporal. However, there appeared to be no area centralis since values in temporoventral and nasodorsal regions were similar. By contrast, a change in location of the area centralis appeared to have taken place in LER7L, with a 180° eye rotation; densities were greater in nasal & temporal compared to dorsal & ventral retina ($P<0{\cdot}01$) and nasally values were higher ($P<0{\cdot}05$) than temporally. No conclusion about the alignment of regional specializations could be drawn for LER9L in which the eye had been rotated by 180°. A visual streak had developed with nasal and temporal densities being significantly ($P<0{\cdot}01$) higher than dorsally and ventrally but no area centralis was indicated since nasal and temporal values were similar.

In *Limnodynastes*, visuotectal projections were visuotopically ordered and rotated to the same extent as the eye itself. Furthermore, the degree of rotation of the visuotectal projection matched that of the area centralis and visual streak (Table 2, compare Fig. 4A,B with Fig. 3E,F). Visual pathways of these animals, assessed from HRP whole brain preparations, were normal. As an exception LER9, with lowest cell densities in the ganglion cell layer, had a visuotopically

disorganized projection arising only from small regions of nasal and temporal visual field. Such projections have previously been described as pattern 1 (Gaze & Jacobson, 1963; Gaze & Keating, 1970; Beazley, 1975). The optic nerve in this animal was thin and its pathway could not be traced.

DISCUSSION

In this paper we have analysed alignment of high density regions, such as the area centralis and visual streak, for the mature retinal ganglion cell layer of Leptodactylid frogs following premetamorphic eye rotations. Stages at which eye rotations were performed were all several months before the area centralis or visual streak would normally become apparent in the ganglion cell layer (Dunlop & Beazley, 1981; Coleman *et al.* 1984). This delay allowed us to test the hypothesis of whether the area centralis and visual streak in *Limnodynastes* or visual streak in *Heleioporus* would be rotated after such surgery.

We have recently reported an autoradiographic study of cell division in mid-larval (NF stage 53/54) *Limnodynastes* as well as for animals at metamorphic climax and juveniles. Results suggested that development of the visual streak was largely a consequence of greater cell division at nasal and temporal ciliary margins than elsewhere, with more cells subsequently entering the ganglion cell layer at these retinal locations. However, the extent of mitosis in temporal retina did not exceed that found nasally, suggesting that formation of the area centralis in temporal retina could not be explained in terms of patterns of cell division alone. Rather, we have argued that lesser growth of the temporal compared to nasal axis may underlie development of this specialization (Coleman *et al.* 1984).

In this study the majority of operated animals developed cell densities whose peak values were within the range of normal and unoperated retinae. It is thus presumed that in these cases the eye anlage was not adversely affected by surgery. For all *Limnodynastes* operated from the time when invagination of the eye cup was virtually complete (NF stage 30/31) and in all *Heleioporus*, cell densities across the ganglion cell layer showed significant regional differences. These observations were consistent with operated retinae having developed an area centralis and visual streak in *Limnodynastes* and a visual streak in *Heleioporus*. However, high cell densities were consistently rotated to the same extent as the eye itself. Thus, determination of adult cell topography in the ganglion cell layer, which as we have argued above probably reflects patterns of cell division and retinal growth, must have already been encoded in the eye anlage. Furthermore, development of specializations in the ganglion cell layer could not be overridden by extraocular cues. In this respect, formation of high density regions in the ganglion cell layer resembles other aspects of eye development such as position of the choroid fissure, pigmentation patterns and extents of cell division at dorsal and ventral ciliary margins. All these anatomical features are intrinsically determined and follow characteristic growth patterns despite displacement of the eye (Sharma &

Hollyfield, 1974, 1980; Jacobson, 1976; Straznicky & Tay, 1977; Gaze *et al.* 1979; Beach & Jacobson, 1979; Katz & Silver, 1981; Munro & Beazley, 1982).

Previous studies have indicated that determination of the location of the choroid fissure and pigmentation patterns is closely linked to specification of central connections. Thus, after embryonic eye rotation, visuotectal projections were rotated to the same extent as these anatomical features (Sharma & Hollyfield, 1974, 1980; Gaze *et al.* 1979; Munro & Beazley, 1982). In this study, alignments of high density regions in the ganglion cell layer and of visuotectal projections were comparable, and also matched the extent to which the eye itself had been rotated. Thus, an association between determination of cell topography in the ganglion cell layer and of visuotectal projections has been indicated. However, the nature of factors governing retinal development and establishment of central connections is little understood. Such influences might include gradients of trophic factors, formation of intercellular junctions and cell adhesiveness (McCaffery, Bennett & Dreher, 1982; Dixon & Cronly-Dillon, 1972; Curtis, 1978; Schlosshauer, Schwarz & Rutishauser, 1984).

In three animals, operated at stages before completion of invagination of the eye cup, cell densities in the ganglion cell layer were depleted. Nevertheless, for two of these animals regional variations in cell density had developed which suggested rotation of high density areas.

Such a reduction in cell density might reflect a lesser generation of cells destined to occupy the ganglion cell layer. Alternatively, normal numbers of cells might have arisen but may subsequently have died. We consider it unlikely that cell division would have been decreased markedly in these animals, since gross cell loss was not apparent in the inner and outer nuclear layers in stained sections of the 11 retinae which had not developed an optic nerve. It is difficult to envisage a fall in mitotic activity at the ciliary margin affecting only precursors of cells destined to occupy the ganglion cell layer. If the normal complement of cells were generated, loss may have resulted from optic axons becoming displaced as they left the eye after early eye rotation (Grant & Rubin, 1982) and subsequently being unable to find connections appropriate for their survival (Beazley & Lamb, 1979). Uncertainty as to the cause of cell depletion in three of our animals precludes conclusions being drawn about development of their cell topography. However, the observation that the *Limnodynastes* with lowest cell densities in the ganglion cell layer (LER9) developed a disorganized projection agrees with studies showing that topography is lost only when ganglion cell densities are very low (Beazley, 1981; Udin & Gaze, 1983).

LDB is a Senior Research Fellow (NH&MRC, Australia). This research was funded by NH&MRC, Australia (grant number 82/0180) and the Muscular Dystrophy Research Association (WA). J. Darby is thanked for expert technical assistance and artwork, H. Jurkiewizc for photographic assistance, L.-A. Coleman for advice on statistics, C. Benson and I. Schlawe for help with typing the manuscript. Dr M. F. Humphrey is thanked for the photographs of *Limnodynastes* embryos. Drs R. Dunlop and C. Masters are gratefully acknowledged for assistance with collecting *Limnodynastes* eggs. Drs R. Tarala and R. Dunlop

are thanked for word-processing facilities and Mrs J. R. Burges for continual support and encouragement.

REFERENCES

BEACH, D. H. & JACOBSON, M. (1979). Patterns of cell proliferation in the developing retina of the clawed frog in relation to blood supply and position of the choroidal fissure *J. comp. Neurol.* **183**, 625–632.

BEAZLEY, L. D. (1975). Factors determining decussation at the optic chiasm by developing retinotectal fibres in Xenopus. *Expl Brain Res.* **23**, 491–504.

BEAZLEY, L. D. (1981). Retinal ganglion cell death and regeneration of abnormal retinotectal projections after removal of a segment of optic nerve in Xenopus tadpoles. *Devl Biol.* **85**, 164–170.

BEAZLEY, L. D. (1984). Formation of specific synaptic connections in the visual system of lower vertebrates. *Current Topics in Research on Synapses* **1**, 53–118.

BEAZLEY, L. D., DARBY, J. E. & PERRY, N. H. (1985). Retinal ganglion cell death during optic nerve regeneration in the frog *Rana pipiens. Neurosci. Lett. Suppl.* **19**, 539.

BEAZLEY, L. D. & LAMB, A. H. (1979). Rerouted axons in Xenopus tadpoles form normal visuotectal projections. *Brain Res.* **179**, 373–378.

BEAZLEY, L. D. & DUNLOP, S. A. (1983). The evolution of an area centralis and visual streak in the marsupial *Setonix brachyurus. J. comp. Neurol.* **216**, 211–231.

COLEMAN, L.-A., DUNLOP, S. A. & BEAZLEY, L. D. (1984). Patterns of cell division during visual streak formation in the frog *Limnodynastes dorsalis. J. Embryol. exp. Morph.* **83**, 119–135.

CURTIS, A. G. (1978). Cell–cell recognition; positioning and patterning systems. *Symp. Soc. exp. Biol.* **32**, 51–82.

DIXON, J. S. & CRONLY-DILLON, J. R. (1972). The fine structure of the developing retina in *Xenopus laevis. J. Embryol. exp. Morph.* **28**, 659–666.

DUNLOP, S. A. & BEAZLEY, L. D. (1981). Changing retinal ganglion cell distribution in the frog *Heleioporus eyrei. J. comp. Neurol.* **202**, 221–236.

DUNLOP, S. A. & BEAZLEY, L. D. (1984). A morphometric study of the retinal ganglion cell layer from metamorphosis in *Xenopus laevis. Vision Res.* **24**, 417–427.

DUNLOP, S. A., HUMPHREY, M. F., COLEMAN, L.-A. & BEAZLEY, L. D. (1983). Specifications of the area centralis and visual streak in the Leptodactylid frog *Limnodynastes dorsalis. Proc. Int. Union Physiol. Science* **XV**: 122.02.

GAZE, R. M., FELDMAN, J. D., COOKE, J. & CHUNG, S.-H. (1979). Orientation of the visuotectal map in Xenopus: developmental aspects. *J. Embryol. exp. Morph.* **53**, 39–66.

GAZE, R. M. & JACOBSON, M. (1963). A study of the retinotectal projection during regeneration of the optic nerve in the frog. *Proc. Roy. Soc. Lond.* **(B) 157**, 420–448.

GAZE, R. M. & KEATING, M. J. (1970). Further studies on the restoration of the contralateral retinotectal projection following regeneration of the optic nerve in the frog. *Brain Res.* **21**, 183–195.

GRANT, P., RUBIN, E. & CIMA, C. (1980). Ontogeny of the retina and optic nerve in *Xenopus laevis.* I. Stages in the early development of the retina. *J. comp. Neurol.* **189**, 593–613.

GRANT, P. & RUBIN, E. (1982). Disruption of optic fibre growth following eye rotation in *Xenopus laevis* embryos. *Nature* **287**, 845–848.

HUMPHREY, M. F. & BEAZLEY, L. D. (1985). Cell death during optic nerve regeneration in the frog *Hyla moorei. J. comp. Neurol.* **236**, 382–402.

HUMPHREY, M. F., DUNLOP, S. A. & BEAZLEY, L. D. (1980). Positional information in the retina is not affected by early embryonic eye rotation in *Limnodynastes dorsalis. Proc. Aust. Physiol. Pharmacol. Soc.* **11**, 90.

JACOBSON, M. (1976). Histogenesis of the retina in the clawed frog with implications for the development of retinotectal connections. *Brain Res.* **103**, 541–545.

JACOBSON, M. (1978). *Developmental Neurobiology.* New York: Plenum Press.

KATZ, M. J. & SILVER, J. (1981). Inverted eye primordia develop into anatomically inverted eyes. *Devl Biol.* **86**, 510–514.

McCaffery, C. A., Bennett, M. R. & Dreher, B. (1982). The survival of neonatal rat retinal ganglion cells *in vitro* is enhanced by the presence of appropriate parts of the brain. *Expl Brain Res.* **48**, 377–386.

Munro, N. S. & Beazley, L. D. (1982). Visuotectal projections following temporary eye transplantation of embryonic eyes to the body in *Xenopus laevis*. *J. Embryol. exp. Morph.* **71**, 97–108.

Nieuwkoop, P. D. & Faber, J. (1956). *Normal table of* Xenopus laevis (*Daudin*). Amsterdam: North Holland Publ.

Schlosshauer, B., Schwarz, U. & Rutishauser, U. (1984). Topological distribution of neural cell adhesion molecule in the developing chick visual system. *Nature* **310**, 141–143.

Sharma, S. C. & Hollyfield, J. G. (1974). Specification of central connections in Rana before appearance of post-mitotic ganglion cells. *J. comp. Neurol.* **155**, 395–408.

Sharma, S. C. & Hollyfield, J. G. (1980). Specification of retinotectal connections during development of the toad *Xenopus laevis*. *J. Embryol. exp. Morph.* **55**, 77–92.

Stone, J. (1981). *The Wholemount Handbook. A Guide to the Preparation and Analysis of Retinal Wholemounts*. Sydney: Maitland Publications Pty. Ltd.

Straznicky, C. & Tay, D. (1977). Retinal growth in double dorsal and double ventral eyes in Xenopus. *J. Embryol. exp. Morph.* **40**, 175–185.

Udin, S. B. & Gaze, R. M. (1983). Expansion and retinotopic order in the goldfish retinotectal map after large retinal lesions. *Expl Brain Res.* **50**, 347–352.

(*Accepted 20 May 1985*)